Modulation of electron energy distributions and discharge parameters in a dual frequency ICP discharge

2013 Plasma Sources Sci. Technol. 22 015022

(http://iopscience.iop.org/0963-0252/22/1/015022)

Plasma Sources Sci. Technol. **22** (2013) 015022 (5pp) doi:10.1088/0963-0252/22/1/015022

Modulation of electron energy distributions and discharge parameters in a dual frequency ICP discharge

Anurag Mishra[1], **Tae Hyung Kim**[1], **Kyong Nam Kim**[1] **and Geun Young Yeom**[1,2]

[1] Department of Advanced Materials Science and Engineering, Sungkyunkwan University, Suwon, Gyeonggi-do 440-746, Korea
[2] SKKU Advanced Institute of Nanotechnology (SAINT), Sungkyunkwan University, Suwon, Gyeunggi-do 440-746, Korea

E-mail: gyyeom@skku.edu

Received 27 September 2012, in final form 3 December 2012
Published 8 January 2013
Online at stacks.iop.org/PSST/22/015022

Abstract

Using a radio frequency (RF) compensated Langmuir probe, modulations in electron energy distribution (EED) and plasma potential are investigated in a discharge produced by a large-area dual frequency/dual antenna inductively coupled plasma source. The discharge is ignited using two frequencies (2 and 13.56 MHz). It is observed that the EEDs can be tailored by varying the power ratio of the two frequencies. Increasing the power level of the low frequency ($P_{2\,\mathrm{MHz}}$) enhances the population density of high-energy electrons; however, increasing the high-frequency power ($P_{13.56\,\mathrm{MHz}}$) increases the low-energy electron population density. At a fixed total power ($P_{2\,\mathrm{MHz}} + P_{13.56\,\mathrm{MHz}}$), the higher the low-frequency power ($P_{2\,\mathrm{MHz}}$) content, the higher the population density of high-energy electrons; however, this trend reverses with high-frequency power ($P_{13.56\,\mathrm{MHz}}$).

The influence of power ratio on plasma density (n_e), plasma temperature (T_e) and plasma potential (V_p) has also been studied. It is found out that the plasma parameters have similar trends with RF power irrespective of its frequency. The value of n_e increases, and T_e and V_p decrease with increasing power. At a fixed $P_{2\,\mathrm{MHz}}$, V_p increases with increasing $P_{13.56\,\mathrm{MHz}}$. However, V_p decreases with increasing $P_{2\,\mathrm{MHz}}$ at a fixed value of $P_{13.56\,\mathrm{MHz}}$.

(Some figures may appear in colour only in the online journal)

1. Introduction

For improving the production efficiency and optimization of fabricating cost of microelectronics devices, large-area plasma sources have become indispensable for future semiconductor and flat panel display manufacturing technologies. This is why the development of large-area plasma sources has become an active area of research in the field of low-temperature plasmas over the last decade [1–6]. According to a technology trend forecast, the semiconductor industry will adopt a wafer diameter of 450 mm within a few years [7]. However, when the wafer size becomes comparable to the wavelength of the excitation frequency ($R \sim \lambda_0$), a standing wave develops in the discharge and produces strong non-uniformity in the plasma species distribution over the wafer area. Therefore, precisely controlling the distribution of discharge species over the wafer area is one of the most technologically challenging issues. Various antenna designs based on different power coupling mechanisms and use of multiple frequencies have been proposed to enhance discharge uniformity over the substrate area [8–10]. Recently, a dual frequency/dual antenna inductively coupled plasma (ICP) source has been proposed to eliminate discharge non-uniformity over the substrate area. This kind of large area ICP source utilizes two radio frequencies of 2 and 13.56 MHz, and a discharge uniformity of ~96% has been achieved using this antenna design [11].

The electron energy distribution function (EEDF) is one of the most important parameters for non-equilibrium low-temperature plasmas. The information extracted from EEDFs is of significant importance in understanding the underlying

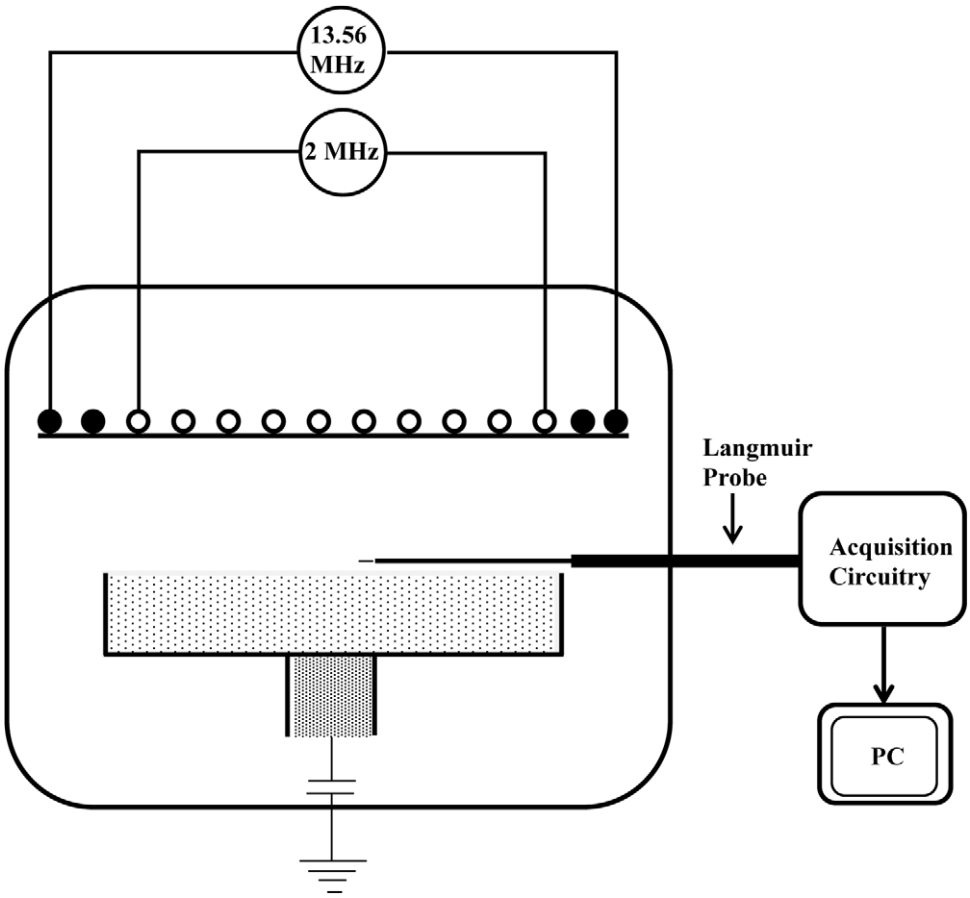

Figure 1. Schematic diagram (not to scale) of the discharge chamber and Langmuir probe system used in this study.

physical and chemical processes occurring in the discharge. It not only provides information about the electron dynamics—the electron heating and energy loss mechanisms—in plasmas, but also defines the discharge mechanisms responsible for the densities of active species (meta-stables, radicals and ions) such as electron impact excitation, dissociation and ionization [13, 14]. The discharge production, sustenance and transport mechanisms change with varying EEDF. Therefore, the EEDF is a very useful control to tailor the discharge properties particular to a specific application.

The dual frequency/dual antenna ICP source operating at 2 and 13.56 MHz not only exhibited a more uniform plasma distribution over the substrate compared with a single frequency antenna ICP operating at 13.56 MHz but also showed improved plasma characteristics such as higher plasma density, lower plasma potential and lower electron temperature [11]. In addition, this kind of antenna design is capable of modulating the EEDF depending on the power levels of both frequencies and can facilitate tuning of the gas dissociation characteristics. In this study, the EEDF measurements, the effect of power levels of both frequencies ($P_{2\,\mathrm{MHz}}$ and $P_{13.56\,\mathrm{MHz}}$) on EEDFs and plasma parameters such as plasma potential, plasma density and electron temperature in dual frequency/dual antenna ICP [11] are presented. The discharge is produced in a CF_4/Ar gas environment which is conventionally used for the etching of semiconductor materials.

2. Experimental set-up

A schematic of the experimental system is illustrated in figure 1. The anodized aluminum chamber used in this study has a cylindrical geometry with inner diameter of 650 mm and height 400 mm. A 35 mm thick quartz window is used to cover the top side of the processing chamber and to hold the ICP source, which consists of two spiral coils. The inner coil (thirteen turns) and outer coil (two turns) are energized by 2 MHz and 13.56 MHz RF powers, respectively. Both RF powers ($P_{2\,\mathrm{MHz}}$ and $P_{13.56\,\mathrm{MHz}}$) are chosen to be 500, 750 and 1000 W. The gases are uniformly distributed inside the chamber via a multi-hole shower head located at the circumference of the vacuum chamber. The separation between the plasma source and the substrate is 130 mm.

The experiments are carried out in an argon (80%, 400 sccm) and CF_4 (20%, 100 sccm) gas environment at a pressure of 10 mTorr. An RF compensated Langmuir probe (supplied by Hiden Analytical Ltd) having a probe tip made of platinum wire, 10 mm in length and 100 μm in diameter, is used. The probe is equipped with a reference electrode and broadband (2–60 MHz) resonance filters to remove RF noise incursion on the current–voltage (I–V) characteristics. The probe is located at the centre and 30 mm above the substrate.

3. Experimental results and discussion

The Druyvesteyn approach is adopted in deriving the EEDFs from the I–V characteristics. According to this, the second derivative of the electron probe current (I_e'') with respect to the probe potential in reference to the plasma potential (V_p–V_b, where V_p is the plasma potential and V_b is the probe potential) is proportional to the EEDF and is obtained numerically by double differentiating as follows:

$$g(\varepsilon) = \frac{2m}{e^3 A}\left(\frac{2\varepsilon}{m}\right)^{1/2} I_e''(\varepsilon). \quad (1)$$

The effective temperature is calculated from the EEDF according to the following relation [15]:

$$\langle\varepsilon\rangle = \frac{1}{n_e}\int_0^\infty g_e(\varepsilon)\,\mathrm{d}\varepsilon, \quad (2)$$

$$T_{\mathrm{eff}} = \tfrac{2}{3}\langle\varepsilon\rangle, \quad (3)$$

where ε, m, e and A are the electron energy, electron mass, electron charge and area of the probe tip, respectively. To eliminate the random noise from the I–V characteristics, a single I–V characteristic is obtained by averaging over 25 scans. To extract the space potential and EEDFs from the I–V characteristics, a MATLAB code is developed and used. The Savitzky–Golay filter, a polynomial of order 3 and data frame length (N_L) of 51, is used to smooth the I–V curves. To eliminate the distortion produced by the Savitzky–Golay filter at the end data points, $(N_L+1)/2$ data points at both data ends are made zero [12].

Figure 2 shows the EEDFs measured at $P_{13.56\,\mathrm{MHz}}$ of 500 W. The $P_{2\,\mathrm{MHz}}$ power is varied from 500 to 1000 W in steps of 250 W. As illustrated in figure 2, all the EEDFs are bi-Maxwellian, typical for low-temperature plasmas at low pressure [15], with two electron temperatures in the non-local kinetic regime [16, 17]. In this regime, the low-energy electrons gain a small amount of energy from collisionless and collisional heating. Under a particular condition ($P_{2\,\mathrm{MHz}}$, $P_{13.56\,\mathrm{MHz}} = 500$ W), the EEDF extends up to 24 eV, and the effective electron temperature (calculated from EEDF according to equation (3)) is 5.9 eV. At a fixed value of $P_{13.56\,\mathrm{MHz}} = 500$ W, as the RF power at low frequency ($P_{2\,\mathrm{MHz}}$) increases from 500 to 1000 W, the EEDFs become more convex, with a greater population density of electrons, suggesting enhanced ionization processes. Additionally, the EEDF extends (24 to 27 eV) towards the high-energy end. Above 12 eV, the EEDF becomes steeper, suggesting cooling of the EEDFs due to electron inelastic collisions, at energies above the collisional inelastic energies ($\varepsilon > \varepsilon^*$) [14].

Figure 3 illustrates the effect of high-frequency power levels ($P_{13.56\,\mathrm{MHz}}$) on the EEDFs, keeping the low-frequency power constant ($P_{2\,\mathrm{MHz}} = 500$ W). From the plot, it can be seen that the EEDFs are bi-Maxwellian, having two groups of electrons with effective electron temperatures of 5.9 eV, when the power $P_{13.56\,\mathrm{MHz}}$ is 500 W. The EEDF becomes more populated with low-energy electrons (<5 eV) as $P_{13.56\,\mathrm{MHz}}$ is increased. However, on the high-energy side, the EEDFs lose

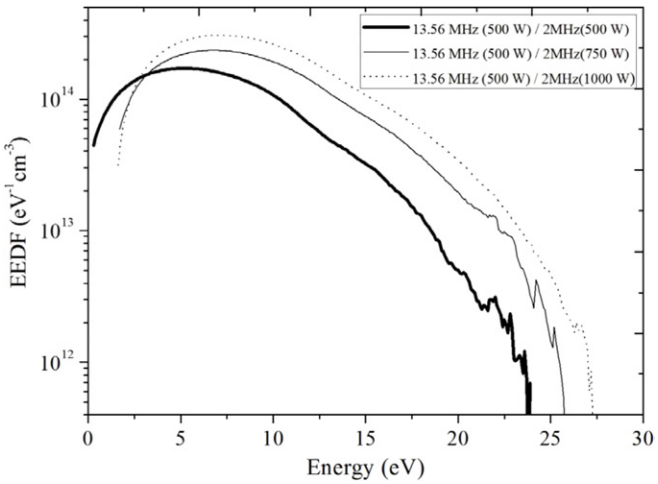

Figure 2. Evolution of electron energy distribution functions with low-frequency power ($P_{2\,\mathrm{MHz}}$) at a pressure of 10 mTorr, in a discharge of Ar(400 sccm)/CF_4(100 sccm). The high-frequency ($P_{13.56\,\mathrm{MHz}}$) power is kept constant at 500 W.

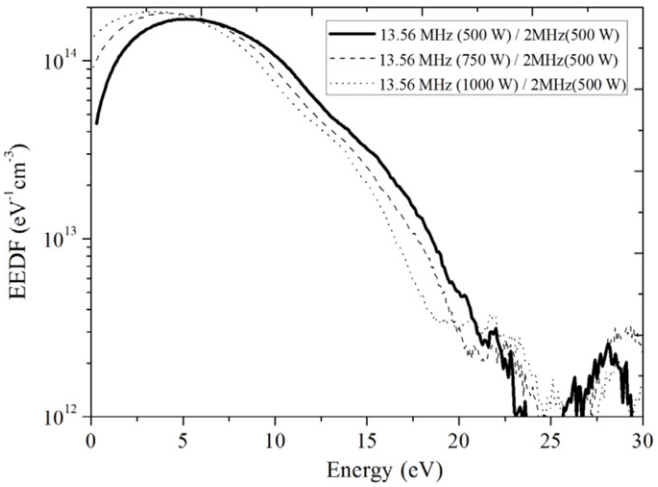

Figure 3. Evolution of electron energy distribution functions with high-frequency power ($P_{13.56\,\mathrm{MHz}}$) at a pressure of 10 mTorr, in a discharge of Ar(400 sccm)/CF_4(100 sccm). The low-frequency power ($P_{2\,\mathrm{MHz}}$) is kept constant at 500 W.

electrons with increasing $P_{13.56\,\mathrm{MHz}}$. Figures 2 and 3 suggest that an efficient tailoring of the EEDF could be achieved using a dual frequency/dual antenna design topology for large-area plasma processing.

To investigate the effect of the RF power ratios of both frequencies ($P_{2\,\mathrm{MHz}}/P_{13.56\,\mathrm{MHz}}$) on the EEDFs at a fixed total power, a series of experiments is carried out. The total power ($P_{2\,\mathrm{MHz}} + P_{13.56\,\mathrm{MHz}}$) is fixed at the two values of 1250 and 1500 W. The measurements shown in figure 4 illustrate that the higher the low-frequency power ($P_{2\,\mathrm{MHz}}$) content, the higher the density of higher energy electrons. In contrast, the higher the high-frequency power ($P_{13.56\,\mathrm{MHz}}$) content, the lower the population density of higher energy electrons; however, with an increase in the low-frequency power ($P_{2\,\mathrm{MHz}}$) the high-energy electron population density increases. This suggests that the low-frequency power ($P_{2\,\mathrm{MHz}}$) is preferentially utilized to produce high energy electrons. With the measurements

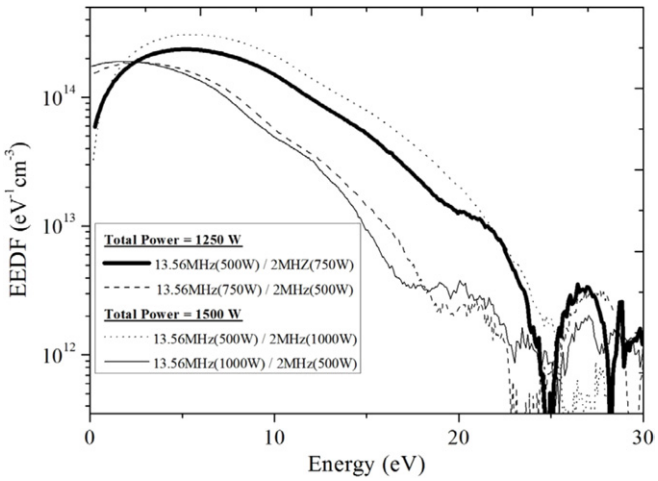

Figure 4. Evolution of electron energy distribution functions at a fixed total power of (*a*) 1250 W and (*b*) 1500 W while varying the RF power ratios of 2 and 13.56 MHz.

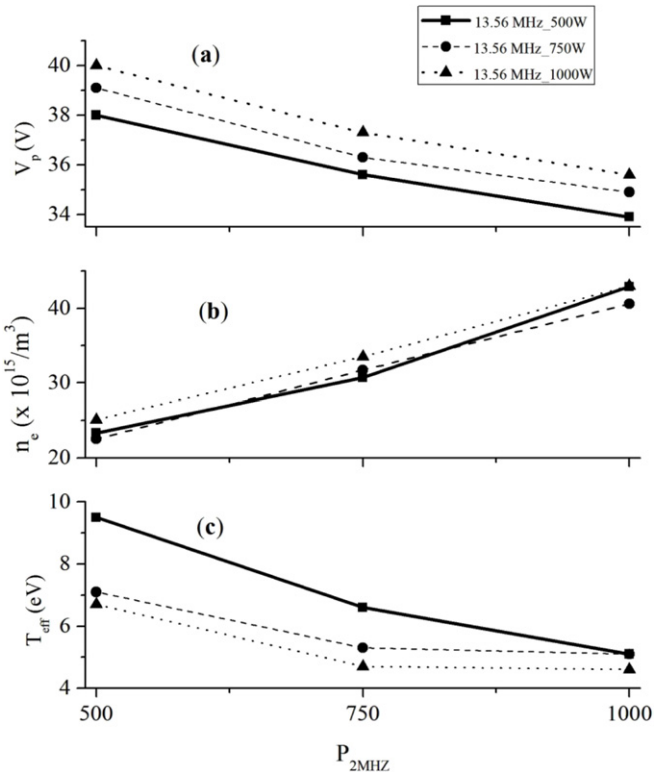

Figure 5. Effect of $P_{2\,\mathrm{MHz}}$ (*a*) plasma potential (*b*) plasma density and (*c*) effective electron temperature at the three chosen values of RF power (500, 750 and 1000 W) of both RF frequency powers.

carried out at a total power of 1500 W, a similar trend, as discussed earlier, is observed.

The effect of $P_{2\,\mathrm{MHz}}$ on the discharge parameters is delineated in figures 5(*a*)–(*c*). Figure 5(*a*) shows the variation of the plasma potential (V_p) with $P_{2\,\mathrm{MHz}}$, at three chosen values (500, 750 and 1000 W) of $P_{13.56\,\mathrm{MHz}}$ and it can be seen that the plasma potential decreases with increasing $P_{2\,\mathrm{MHz}}$. This could be due to a decrease in electron temperature (T_e) and increase in plasma density, shown in figure 5(*b*). Figure 5(*c*) shows the variation in effective electron temperature (T_eff)

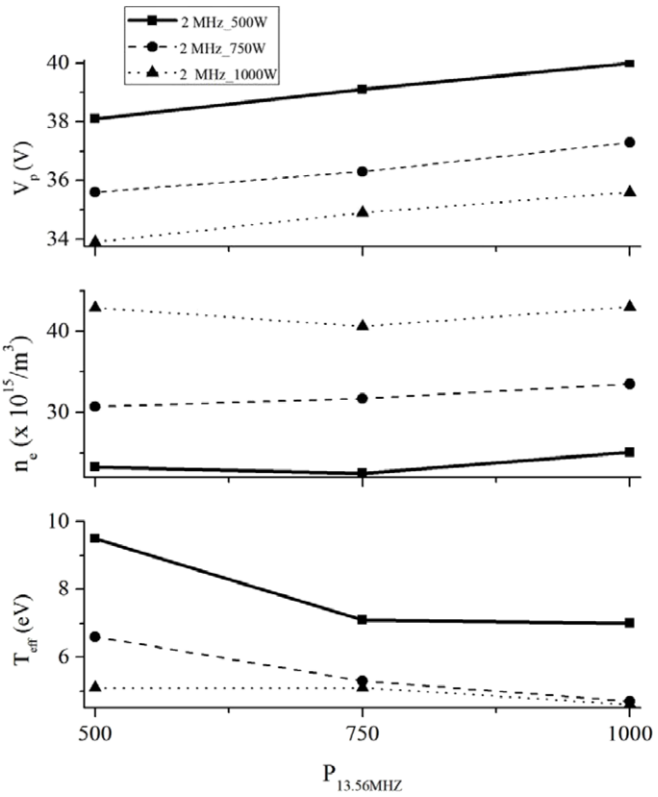

Figure 6. Effect of $P_{13.56\,\mathrm{MHz}}$ (*a*) plasma potential (*b*) plasma density and (*c*) effective electron temperature at the three chosen values of RF power (500, 750 and 1000 W) of both RF frequency powers.

with $P_{2\,\mathrm{MHz}}$. This observed trend of T_eff is typical for low-temperature plasmas caused by enhanced multistep ionization. Figure 6(*a*) illustrates the V_p dependence on $P_{13.56\,\mathrm{MHz}}$. From figure 5(*b*), it can be seen that V_p increases with $P_{13.56\,\mathrm{MHz}}$ at a fixed value of $P_{2\,\mathrm{MHz}}$ due to increased potential on the outer coil (increased sheath potential by capacitive coupling) [11]. This shows that the plasma potential, and thus ion bombarding energy, can be modulated by adjusting the RF power levels on both coils. Figures 6(*b*) and (*c*) depict the dependence of the n_e and T_eff on $P_{13.56\,\mathrm{MHz}}$. The value of n_e increases slightly with $P_{13.56\,\mathrm{MHz}}$; however, T_eff decreases with increasing $P_{13.56\,\mathrm{MHz}}$. The influence of $P_{13.56\,\mathrm{MHz}}$ on the plasma parameters is not very pronounced because the measurements are carried out at the centre of discharge, far (∼200 mm) from the 13.56 MHz coil, which is located at the boundary of the ICP source.

4. Conclusion

In this study, it is demonstrated that electron energy distribution functions (EEDFs) and discharge parameters can be modulated effectively by adjusting the separate RF power levels on both coils of a dual frequency/dual antenna ICP source. Therefore, this design of ICP antenna not only produces a discharge with very high uniformity over the wafer area but also provides a control to modulate the EEDFs and plasma parameters in the bulk discharge.

Acknowledgments

This work was supported by the IT R&D Program of MKE (2009-S-007-1, development of 300 mm wafer backend processing equipment for 32 nm node semiconductor devices). This work was also supported in part by the World Class University program of the National Research Foundation of Korea (Grant No R32-2008-000-10124-0) and by the Ministry of Education, Science and Technology (2010-0015035).

References

[1] Chang T H, Chen N C, Chao H W, Lin J C, Huang C C and Chen C C 2012 *Phys. Plasmas* **19** 033302
[2] Kim K N, Lim J H, Jeong H B, Yeom G Y, Lee S H and Lee J K 2012 *Microelectron. Eng.* **89** 133
[3] Se-Geun Park, Chul Kim and Beom-hoan O 1999 *Thin Solid Films* **355–356** 252
[4] Chang C Y and Sze S M 1996 *ULSI Technology* (New York: McGraw-Hill) p 329
[5] Hopwood J 1992 *Plasma Sources Sci. Technol.* **1** 109
[6] Kahoh M, Suzuki K, Tonotani J, Aoki K and Yamage M 2001 *Japan. J. Appl. Phys.* **40** 5419
[7] International Technology Roadmap for Semiconductors, 2009 edition http://www.itrs.net
[8] Yang and Kushner M J 2010 *J. Appl. Phys.* **108** 113306
[9] Hong S P, Lim J H, Gweon G H and Yeom G Y 2010 *Japan. J. Appl. Phys.* **49** 080217
[10] Kim K N, Lim J H, Yeom G Y, Lee S H and Lee J K 2006 *Appl. Phys. Lett.* **89** 251501
[11] Mishra A, Kim K N, Kim T H and Yeom G Y 2012 *Plasma Sources Sci. Technol.* **21** 035018
[12] Magnus F and Gudmundsson J T 2008 *Rev. Sci. Instrum.* **79** 073503
[13] Godyak V A 2006 *IEEE Trans. Plasma Sci.* **34** 755–66
[14] Aanesland A, Berdin J, Chabert P and Godyak V 2012 *Appl. Phys. Lett.* **100** 044102
[15] Lieberman M A and Lichtenberg A J 2004 *Principle of Plasma Discharges and Materials Processing* 2nd edn (New York: Wiley)
[16] Godyak V A and Piejak R B 1990 *Phys. Rev. Lett.* **65** 996
[17] Lee H C, Lee M H and Chung C W 2010 *Appl. Phys. Lett.* **96** 041503